Title page

Title: Using Volumetric Multispectral Optoacoustic Tomography (vMSOT) for Three-Dimensional (3D) Reconstruction of Skin Tumors – A Further Evaluation with Histopathological Correlation.

Sai Yee Chuah[1†], Amalina Binte Ebrahim Attia[2†], Chris Jun Hui Ho[2], Xiuting Li[2], Joyce Siong-See Lee[1], Melissa Wee Ping Tan[1], Angeline Anning Yong[1], Aaron Wei Min Tan[1], Daniel Razansky[3], Malini Olivo[2], Steven Tien Guan Thng[1]

[1] National Skin Centre, Singapore

[2] Lab of Bio-optical Imaging, Singapore Bioimaging Consortium, A*STAR, Singapore

[3] Institute for Biological and Medical Imaging, Technical University of Munich and Helmholtz Center Munich, Germany

[†]Contributed equally

Article type: Letter to the Editor

Author names and affiliations:

Dr Sai Yee Chuah

MBChB (Glasgow), MRCP (UK), MRCPS (Glasgow), Diploma in Dermatology (RCPSG), FAMS (Dermatology)

Consultant

Department of Dermatology, National Skin Centre, 1 Mandalay Road, Singapore. 308205.

E-mail: sychuah@nsc.com.sg

Dr Amalina Binte Ebrahim Attia

PhD

Research Fellow, Scientist

Lab of Bio-optical Imaging, Singapore Bioimaging Consortium, A*STAR, Singapore

Email: Amalina_Attia@sbic.a-star.edu.sg

Dr Chris Jun Hui Ho

PhD

Research Fellow, Scientist

Lab of Bio-optical Imaging, Singapore Bioimaging Consortium, A*STAR, Singapore

Email: chris_ho@sbic.a-star.edu.sg

Dr Xiuting Li

PhD

Research Fellow, Scientist

Lab of Bio-optical Imaging, Singapore Bioimaging Consortium, A*STAR, Singapore

Email: li_xiuting@sbic.a-star.edu.sg

Dr Siong See Joyce Lee

MBBS, MRCP (UK), M Med (Int Med), FAMS Dip Dermatopathology (ICDP-UEMS)

Senior Consultant

Department of Dermatology, National Skin Centre, 1 Mandalay Road, Singapore. 308205.

Email: joycelee@nsc.com.sg

Dr Wee Ping Melissa Tan

MBBS, MRCP (UK), FAMS

Senior Consultant

Department of Dermatology, National Skin Centre, 1 Mandalay Road, Singapore. 308205.

E-mail: wptan@nsc.com.sg

Dr Anning Angeline Yong

MBBS, MRCP (UK), MRCS (Edin), FRCP (Edin), FAMS (Dermatology)

Consultant

Department of Dermatology, National Skin Centre, 1 Mandalay Road, Singapore. 308205.

E-mail: angelineyong@nsc.com.sg

Dr Wei Min Aaron Tan

MBBS, FAMS (Dermatology), MRCP (UK), MRCPS (Glasg)

Consultant

Department of Dermatology, National Skin Centre, 1 Mandalay Road, Singapore. 308205.

E-mail: aarontan@nsc.com.sg

Prof Daniel Razansky

Institute for Biological and Medical Imaging, Technical University of Munich and Helmholtz Center Munich, Germany

Email: dr@tum.de

Prof Malini Olivo

Head, Bio-Optical Imaging Group, Scientist

Lab of Bio-optical Imaging, Singapore Bioimaging Consortium, A*STAR, Singapore

Email: Malini_Olivo@sbic.a-star.edu.sg

A/Prof Tien Guan Steven Thng

MBBS, MRCP (UK), FRCP (Edin)

Senior Consultant

Department of Dermatology, National Skin Centre, 1 Mandalay Road, Singapore. 308205.

E-mail: steventhng@nsc.com.sg

Name of institution at which research was conducted: Department of Dermatology, National Skin Centre, 1 Mandalay Road, Singapore. 308205.

Corresponding Author:

A/Prof Tien Guan Steven Thng

MBBS, MRCP (UK), FRCP (Edin)

Senior Consultant

Department of Dermatology, National Skin Centre, 1 Mandalay Road, Singapore. 308205.

E-mail: steventhng@nsc.com.sg

Prof Malini Olivo

Head, Bio-Optical Imaging Group, Scientist

Lab of Bio-optical Imaging, Singapore Bioimaging Consortium, A*STAR, Singapore

Email: Malini_Olivo@sbic.a-star.edu.sg

Prof Daniel Razansky

Institute for Biological and Medical Imaging, Technical University of Munich and Helmholtz Center Munich, Germany

Email: dr@tum.de

Short title: Volumetric MSOT imaging of non-melanoma skin cancers

Article key words: photoacoustic imaging, non-invasive; 3D imaging, non-melanoma skin cancer, histology

Abbreviations used: BCC, basal cell carcinoma; MMS, Moh's micrographic surgery; MSOT, multispectral optoacoustic tomography; NMSC, non-melanoma skin cancer; SCC, squamous cell carcinoma

Manuscript word count (excluding abstract and references): 997

Table count: 0

Figure count: 2

Supplementary Material: 1

Number of References: 13

Funding sources for the work: This work was supported by intramural funding from Singapore Bioimaging Consortium, Biomedical Research Council of Agency for Science, Technology and Research (A*STAR).

Financial disclosure: None reported

Financial interest: The authors declare that there are no financial interests.

Conflict of interest: The authors have no conflict of interest to declare.

NHG DSRB Reference: 2015/00462 (Approved IRB)

TO THE EDITOR

Surgical extirpation is the most effective method to treat non-melanoma skin cancers (NMSC) but it is usually cosmetically undesirable due to the large safety margins (Gualdi et al., 2015, Vuyk and Lohuis, 2001). Mohs micrographic surgery (MMS) is ideal but is time consuming (Tolkachjov et al., 2017). Thus, there is a clinical need for a preoperative imaging tool to guide surgery and map deep penetrating NMSC in 3D. Skin cancer screening may begin with the aid of adjunctive tools for diagnosis, such as dermoscopy and reflectance confocal microscopy (RCM)(Guitera et al., 2012, Malvehy and Pellacani, 2017), optical coherence tomography (OCT),(Mogensen et al., 2009) and the sequential treatment. These imaging tools however, lack penetration depth and specificity, making it unsuitable to differentiate certain skin structures clearly e.g. melanin and blood vessels (Guilera et al., 2016).

We have demonstrated the first clinical use of volumetric multispectral optoacoustic tomography (vMSOT) equipped with handheld detectors for 3D reconstruction of skin tumors in a pilot study (Figure S1)(Attia et al., 2017, Chuah et al., 2017). It is a label-free non-invasive imaging technique based on real-time optoacoustic sensing of tissue absorbers (including hemoglobin, melanin and lipids) emitting ultrasound vibrations from absorption of photons from a laser beam (Ford et al., 2016). Due to the distinct absorption profiles of the absorbers, vMSOT is able to spatially map the distribution of these bio-chromophores in a volumetric 3D space to give morphology and vasculature information of these cutaneous lesions. The vMSOT images are reconstructed in 3D in minutes, unmixed for absorbers, saved as 2D image stacks and 3D rendering can be performed within seconds on a typical desktop. We aim to evaluate the reliability of vMSOT in the assessment of NMSC dimensions by correlating with histological measurements of surgically resected NMSC for its proposed use as a pre-operative delineation of

neoplastic skin conditions. The vMSOT dimensions of the lesions were measured based on their melanin or hemoglobin spectral signatures, depending on the lesion's pigmentation in a mixed ethnicity population. Patients' demographic (Table S1), methodologies, image processing details are described in the Supplementary Materials online.

In one representative basal cell carcinoma (BCC); patient 19 (Figure 1A-C, Table S1), vMSOT images of the BCC were acquired showing the lateral views and its 3D projection (Figure 1D). Distributions of the melanin and oxy-hemoglobin signals representing blood vessels were apparent. The tumor dimensions were then extracted from both melanin and hemoglobin signal distributions along the longest and deepest infiltration axes represented as the dotted white lines to give tumor length; 7.42 mm (Figure 1E) and depth; 3.04 mm (Figure 1F); correlating well with the excision length of 8.13 mm and depth of 2.50 mm.

Different subtypes of BCC on different skin phototypes were studied. Patient 17 with Fitzpatrick skin type II presented with an erythematous BCC plaque on his forehead (Figure 1G-I). Most BCCs appear pigmented in people of color (Gloster and Neal, 2006, Kim et al., 2009) such as patient 20 (Fitzpatrick type IV) (Figure 1J-L). Because vMSOT can differentiate the spectral signatures of oxy- and deoxy-hemoglobin from melanin, both pigmented and non-pigmented NMSCs can be imaged with vMSOT. The erythematous nature of the BCC on patient 17 was shown as a strong congregation of oxy-hemoglobin signals on the superficial skin surface (Figure 1G) compared to the adjacent normal skin whereby the dermal vasculature was ordered (Figure S2).

A statistically significant correlation for both tumor depth and length was found between vMSOT and histological analysis ($r = 0.90$, $p < 0.0001$ and $r = 0.85$, $p < 0.0001$ respectively, Figure 2A-B). The Bland-Altman plots showed that the lower and upper limits of agreement

between the two measurement techniques of tumor depth were −1.47 mm and 0.76 mm, respectively, while they were -2.95 mm and 1.35 mm respectively for tumor length (Figure 2C-D). The Bland–Altman data also suggest that the tumor depth measurements agreed better than tumor length with a smaller standard deviation (0.57 vs. 1.10 mm for tumor depth and length respectively). No significant difference was found between the differences in measurements between histology and vMSOT via excision and MMS surgeries. The differences in measurements between histology and vMSOT showed no significance bias towards the type of surgery (p = 0.17 and p = 0.38, tumor depth and length respectively, Fig 2E-F) and type of NMSC (p = 0.70 for tumor depth, Figure S3). Notably, there were only a few cases of SCC represented in the statistical analysis as only 20% of all NMSCs are SCCs (Eisemann et al., 2014).

Our results show that vMSOT is accurate in measuring tumor dimensions irrespective of the different types of NMSCs and skin phototype. However, the accuracy is limited by the field of view (FOV) of the vMSOT scanner and if the tumor is too superficial (<0.5 mm). Case 22 reported a histologic depth of 0.47 mm, indicating that vMSOT was less accurate at very shallow depths, which can be attributed to the unisotropic resolution at the peripheral regions of the FOV of the matrix array detector (Ford et al., 2016). The lower detection limit of the vMSOT may lie between 0.47 and 1.28 mm, the latter being the smallest depth measured by vMSOT in this study (Table S1). In case 16, the tumor depth measured by vMSOT exceeded the histologic measurement by a factor of ~5 (Table S1). The disparity between the measurements may be attributed to the raised scaly plaque of the BCC which may be present during the vMSOT imaging, but could have dropped off during histological processing.

Case 18 which lie below the lower limit of agreement of tumor length yielded a vMSOT measurement twice the tumor length compared to its histologic equivalent. The ulceration and raised edges of the tumor coupled with its inaccessible location between the nose and lip could have contributed to the discrepancy (Figure S4A). Notably, the vMSOT depth was measured from the skin surface to the vascular structure, which corresponded to MMS depth. Visualizing the macrovasculature surrounding the NMSC may aid in the complete removal of the tumor.

The limitations of this study include the relatively small sample size, although it is generally sufficient to determine the agreement of tumor dimensions between the histologic and vMSOT measurements. Additionally, the effective FOV of the MSOT configuration is 10 x 10 x 12 mm and the geometry of the vMSOT handheld probe can make it difficult accessing certain curved areas on the face; limiting the number of NMSC that could be studied.

The demonstration of vMSOT accuracy in determining the tumor dimensions is pertinent, reinforcing the potential of its pre-operative use in aiding dermatologic surgeons in margin demarcations to reduce the number of steps required in MMS. Furthermore, vMSOT offers a unique volumetric approach in visualizing the tumors non-invasively, thus offering significant diagnostic value.

CONFLICT OF INTEREST

The authors declare no conflicts of interest.

ACKNOWLEDGEMENTS

This work was supported by intramural funding from Singapore Bioimaging Consortium, Biomedical Research Council of Agency for Science, Technology and Research (A*STAR).

REFERENCES

Attia ABE, Chuah SY, Razansky D, Ho CJH, Malempati P, Dinish U, et al. Noninvasive real-time characterization of non-melanoma skin cancers with handheld optoacoustic probes. Photoacoustics 2017;7:20-6.

Chuah S, Attia A, Long V, Ho C, Malempati P, Fu C, et al. Structural and functional 3D mapping of skin tumours with non-invasive multispectral optoacoustic tomography. Skin Research and Technology 2017;23(2):221-6.

Eisemann N, Waldmann A, Geller AC, Weinstock MA, Volkmer B, Greinert R, et al. Non-melanoma skin cancer incidence and impact of skin cancer screening on incidence. Journal of Investigative Dermatology 2014;134(1):43-50.

Ford SJ, Bigliardi PL, Sardella TC, Urich A, Burton NC, Kacprowicz M, et al. Structural and functional analysis of intact hair follicles and pilosebaceous units by volumetric multispectral optoacoustic tomography. Journal of Investigative Dermatology 2016;136(4):753-61.

Gloster HM, Neal K. Skin cancer in skin of color. Journal of the American Academy of Dermatology 2006;55(5):741-60.

Gualdi G, Monari P, Apalla Z, Lallas A. Surgical treatment of basal cell carcinoma and squamous cell carcinoma. G Ital Dermatol Venereol 2015;150(4):435-47.

Guilera JM, Capurro AB, Alvárez CC, Sardá SP. The role of reflectance confocal microscopy in clinical trials for tumor monitoring. Dermatologic clinics 2016;34(4):519-26.

Guitera P, Menzies SW, Longo C, Cesinaro AM, Scolyer RA, Pellacani G. In vivo confocal microscopy for diagnosis of melanoma and basal cell carcinoma using a two-step method: analysis of 710 consecutive clinically equivocal cases. Journal of investigative dermatology 2012;132(10):2386-94.

Kim GK, Del Rosso JQ, Bellew S. Skin cancer in Asians: part 1: nonmelanoma skin cancer. The Journal of clinical and aesthetic dermatology 2009;2(8):39.

Malvehy J, Pellacani G. Dermoscopy, Confocal Microscopy and other Non-invasive Tools for the Diagnosis of Non-Melanoma Skin Cancers and Other Skin Conditions. Acta dermato-venereologica 2017;97.

Mogensen M, JOERGENSEN T, Nürnberg BM, Morsy HA, Thomsen JB, Thrane L, et al. Assessment of optical coherence tomography imaging in the diagnosis of non-melanoma skin cancer and benign lesions versus normal skin: observer-blinded evaluation by dermatologists and pathologists. Dermatologic Surgery 2009;35(6):965-72.

Tolkachjov SN, Brodland DG, Coldiron BM, Fazio MJ, Hruza GJ, Roenigk RK, et al. Understanding Mohs Micrographic Surgery: A Review and Practical Guide for the Nondermatologist. Mayo Clinic Proceedings: Elsevier; 2017. p. 1261-71.

Vuyk H, Lohuis P. Mohs micrographic surgery for facial skin cancer. Clinical Otolaryngology 2001;26(4):265-73.

Fig 1. Basal cell carcinoma on the left cheek of patient 19. (A) Clinical image of lesion showing heterogeneous pigmented nodule; (B) H&E staining photomicrograph of lesion after excision showing nodules of basaloid cells; (C) Reflectance confocal microscopy image of the lesion during diagnosis showing nests of tumor cells in the dermis with bright white spots indicating melanin; (D) Maximum intensity projections of the volumetric MSOT images in different projections (xy, yz and xz) and the 3D projection of the lesion. Yellow signals indicate melanin in the lesion while the red signals indicate the oxy-hemoglobin representing blood vessels in the lesion. The white lines drawn indicate the distance from which the collective MSOT signals were plotted shown in for tumor (E) length and (F) depth. The tumor length and depth were then determined from the distance between the non-baseline values of the plot; a.u. − arbitrary units. (G-L) Basal cell carcinoma cases on patients 17 and 20. Maximum intensity projections of the volumetric MSOT images of BCC cases in (G, H) Caucasian patient with Fitzpatrick skin type II (Patient 17) and (J, K) Asian patient with Fitzpatrick skin type IV (Patient 20). The maximum intensity projections show the different views of the skin lesion from the top (xy) top and their cross-sectional views (yz and xz). The clinical image of BCC on (H) Patient 17 showed an erythemous plaque (blue arrow) on the left forehead while the BCC on (K) Patient 20 appeared as a pigmented plaque on the right forehead. The black scale bars indicate 10 mm. The three-dimensional MSOT rendering of both BCCs in (I) Fitzpatrick skin type II skin (Patient 17) and (L) Fitzpatrick skin type IV skin (Patient 20) are also shown. The BCCs were removed via Moh's micrographic surgery.

Fig 2. Scatter plot of measurements of tumor (A) depth and (B) length by histology and MSOT in the same tumor samples. The solid line indicates the regression line of the plot while the dotted line indicates perfect agreement as reference. Less variability is seen between histological and MSOT measurements of tumor depth compared with their measurements of tumor length. Bland-Altman plot shows agreement of tumor (C) depth and (D) length measurements in histologic specimen (reference standard) and by MSOT imaging. The differences between the two techniques are plotted against the means of measurements from the two techniques. One out of 25 tumors (4%) lie outside the limits of agreement for tumor depth; mean difference, –0.02 mm; 95% limits of agreement, –1.08 mm, 1.13 mm. One out of 20 tumors (5%) lie outside the limits of agreement for tumor length; mean difference, –0.121 mm; 95% limits of agreement, –2.62 mm, 2.38 mm. The dashed lines indicate the limits of agreements and the solid line represent the mean difference in measurements between the two techniques; Scatter plot display of the differences in measurements between histology and MSOT in tumor (E) depth and (F) length to test the bias on the method of surgery represented. The lines represents the mean and SD values of each scatter plot.

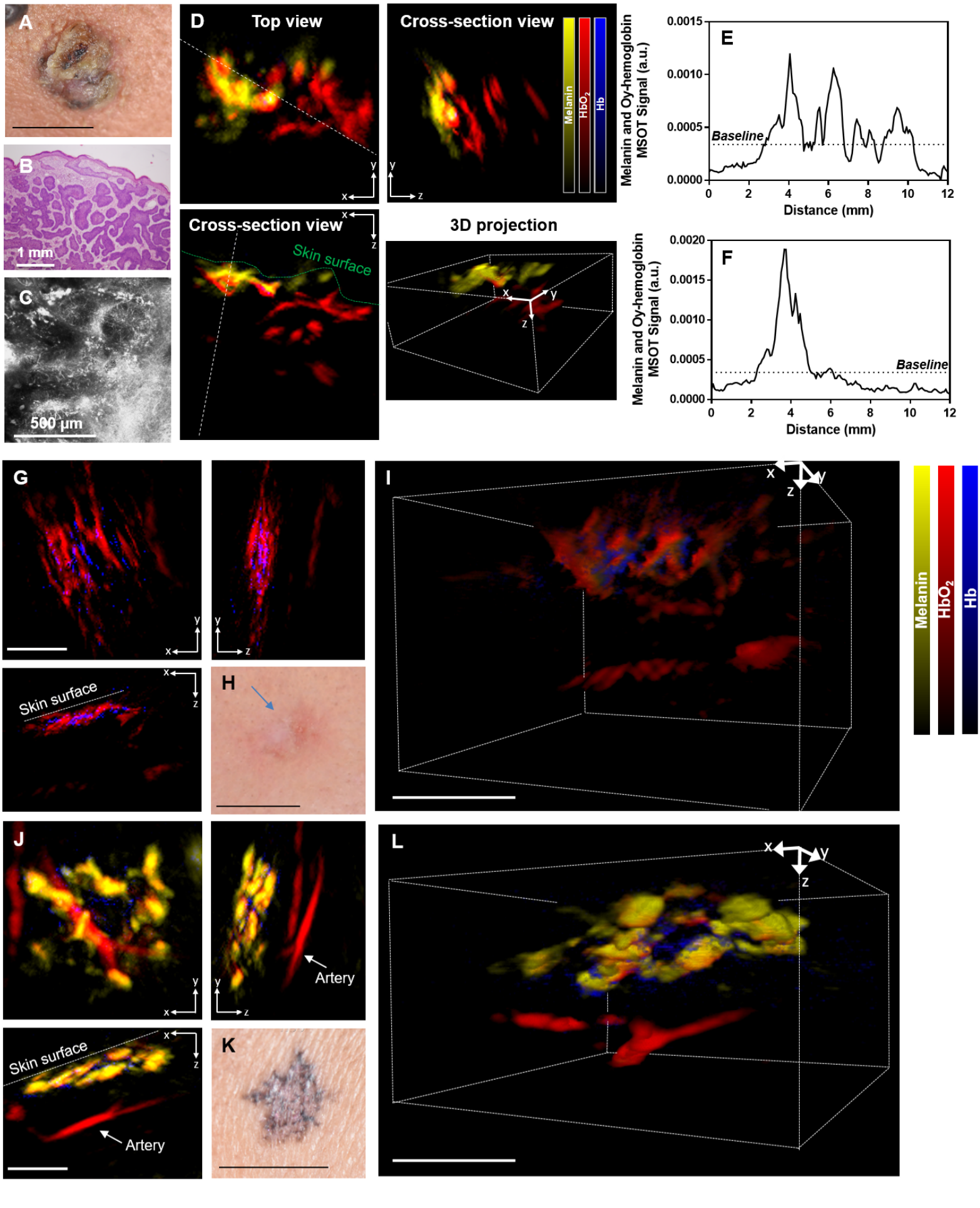
A
B
1 mm
C
500 μm
D
Top view
Cross-section view
Melanin
HbO2
Hb
Cross-section view
Skin surface
3D projection
E
Melanin and Oy-hemoglobin MSOT Signal (a.u.)
0.0015
0.0010
0.0005
0.0000
Baseline
0 2 4 6 8 10 12
Distance (mm)
F
Melanin and Oy-hemoglobin MSOT Signal (a.u.)
0.0020
0.0015
0.0010
0.0005
0.0000
Baseline
0 2 4 6 8 10 12
Distance (mm)
G
Skin surface
H
I
Melanin
HbO2
Hb
J
Artery
Skin surface
Artery
K
L

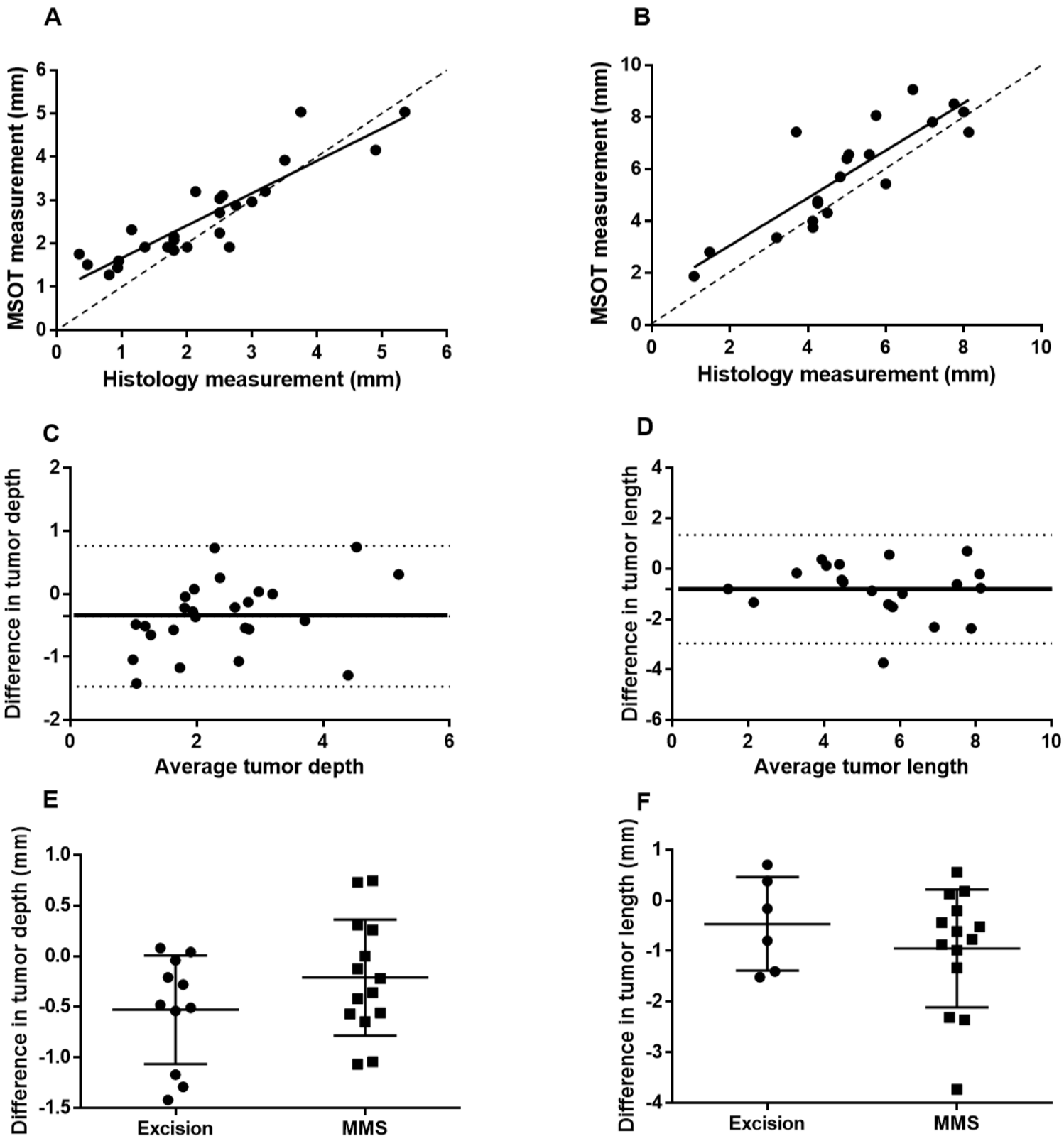
A
MSOT measurement (mm)
Histology measurement (mm)
B
MSOT measurement (mm)
Histology measurement (mm)
C
Difference in tumor depth
Average tumor depth
D
Difference in tumor length
Average tumor length
E
Difference in tumor depth (mm)
Excision
MMS
F
Difference in tumor length (mm)
Excision
MMS

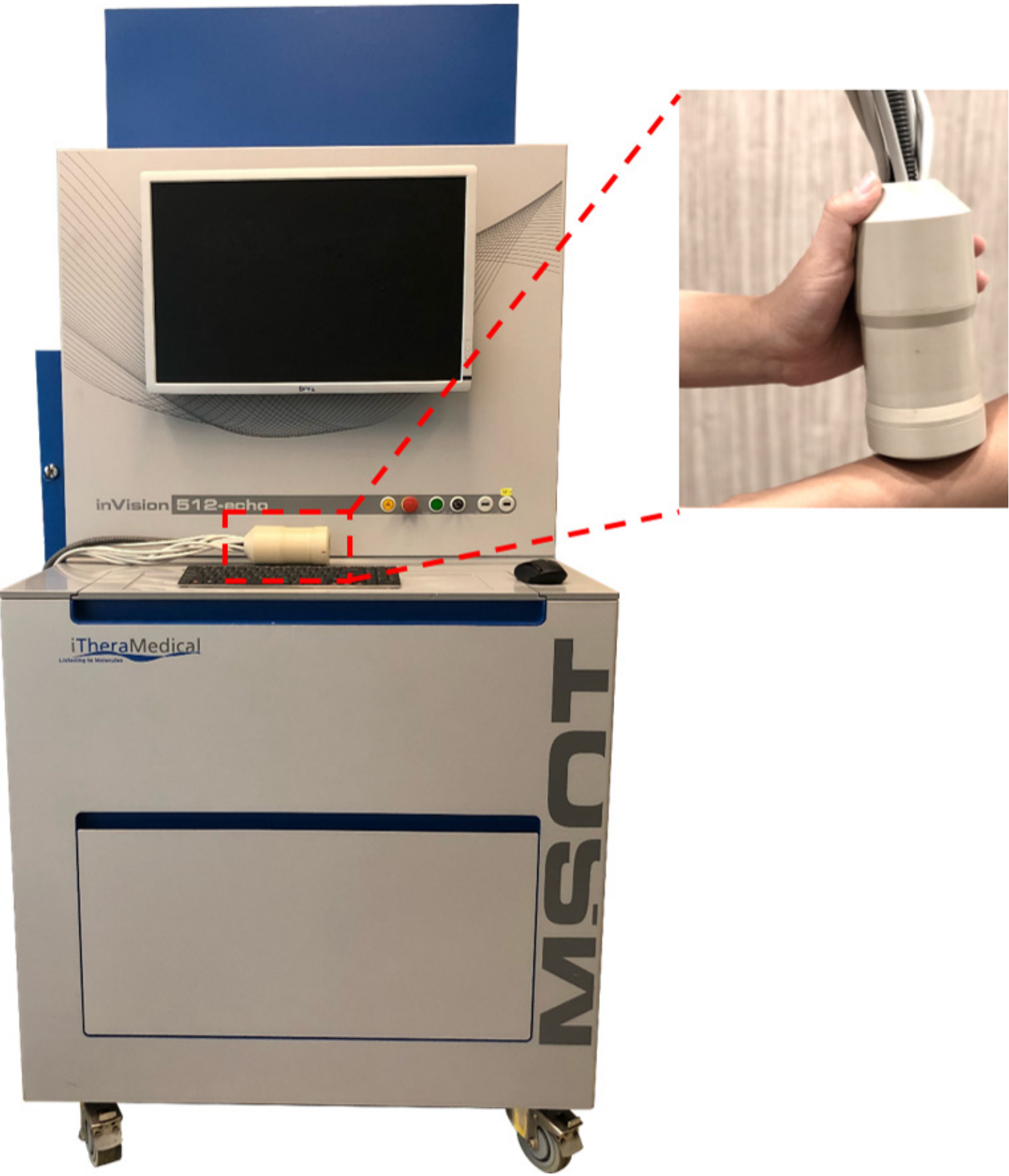
inVision 512-echo
iTheraMedical
MSOT